HHS Public Access

Author manuscript

Cell Rep. Author manuscript; available in PMC 2017 August 23.

Published in final edited form as:

Cell Rep. 2017 July 05; 20(1): 89–98. doi:10.1016/j.celrep.2017.06.024.

Time-resolved fast mammalian behavior reveals complexity of protective pain responses

Liam E. Browne[1,6,*], **Alban Latremoliere**[2], **Brendan P. Lehnert**[3], **Alyssa Grantham**[2], **Catherine Ward**[2], **Chloe Alexandre**[4], **Michael Costigan**[2,5], **Frédéric Michoud**[2], **David P. Roberson**[2], **David D. Ginty**[3], and **Clifford J. Woolf**[2,*]

[1]Kirby Neurobiology Center, Boston Children's Hospital and Department of Neurobiology, Harvard Medical School, Boston, MA 02115, USA; Wolfson Institute for Biomedical Research, University College London, London WC1E 6BT, UK

[2]Kirby Neurobiology Center, Boston Children's Hospital and Department of Neurobiology, Harvard Medical School, Boston, MA 02115, USA

[3]Howard Hughes Medical Institute, Department of Neurobiology, Harvard Medical School, Boston, MA 02115, USA

[4]Department of Neurology, Beth Israel Deaconess Medical Center and Department of Neurobiology, Harvard Medical School, Boston, MA 02115, USA

[5]Department of Anesthesia, Boston Children's Hospital, Boston, MA 02115, USA

SUMMARY

Potentially harmful stimuli are detected at the skin by nociceptor sensory neurons that drive rapid protective withdrawal reflexes and pain. We set out to define at a millisecond timescale the relationship between the activity of these sensory neurons and the resultant behavioral output. Brief optogenetic activation of cutaneous nociceptors was found to activate only a single action potential. This minimal input was used to determine high-speed behavioral responses in freely-behaving mice. The localised stimulus generated widespread dynamic repositioning and alerting sub-second behaviors whose nature and timing depended on the context of the animal, its position, activity and alertness. Our findings show that the primary response to injurious stimuli is not limited, fixed or localized, but is dynamic, and involves recruitment and gating of multiple circuits distributed throughout the central nervous system at a sub-second time scale to effectively both alert to the presence of danger and minimize risk of harm.

[*]Correspondence to: liam.browne@ucl.ac.uk (L.E.B.), clifford.woolf@childrens.harvard.edu (C.J.W.).
[6]Lead contact

AUTHOR CONTRIBUTIONS

Conceptualization, L.E.B. and C.J.W.; Methodology, L.E.B. and C.J.W.; Investigation, L.E.B., A.L., B.P.L, A.G., C.W., C.A., and M.C.; Formal Analysis, L.E.B., A.L., B.P.L., C.A.; Resources, L.E.B, D.P.R. and F.M.; Validation, A.G., and C.W.; Writing – Original Draft, L.E.B. and C.J.W.; Writing – Review & Editing, L.E.B., A.L., B.P.L, M.C., F.M., D.D.G. and C.J.W.; Visualization, L.E.B., A.L., and C.J.W.; Funding Acquisition, L.E.B. and C.J.W.; Supervision, L.E.B. and C.J.W.

Graphical abstract

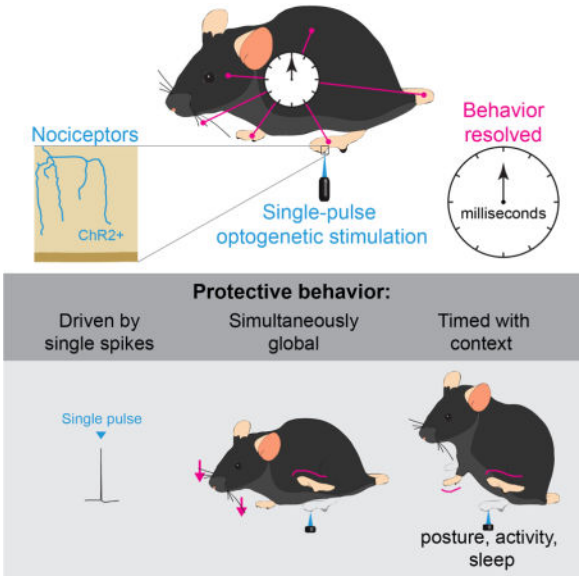

Keywords

Pain; nociception; reflexes; quantitative behavior; optogenetics

INTRODUCTION

Potentially damaging noxious stimuli activate high-threshold primary afferent neurons, the nociceptors, which include sensory neurons with thinly myelinated (Aδ) or unmyelinated (C) axons (Julius, 2013; Prescott et al., 2014; Woolf, 1983). In a series of seminal studies that represented the first analysis of circuits in the central nervous system, Sir Charles Sherrington showed that cutaneous nociceptors activate spinal reflex arcs to drive the withdrawal of an affected limb from the potential source of harm (Sherrington, 1910). Subsequent work by Schouenborg and colleagues found that each motor pool has distinctive excitatory and inhibitory cutaneous receptive fields to produce a hindlimb movement specific to a precise stimulation site, the “modular” theory of withdrawal reflex organization (Schouenborg and Kalliomaki, 1990; Schouenborg and Weng, 1994). Nociceptive withdrawal reflexes are considered the basic unit of protective pain-related behavior and are presumed to represent amongst the simplest polysynaptic relationship between sensory input and motor output (Clarke and Harris, 2004). These protective responses need to be rapid and yet coordinated appropriately. However, the relationship between a purely nociceptive stimulus and the global resultant behavior has not been studied with high temporal resolution.

How do nociceptor inputs initiate rapid behaviors that are most appropriate for dealing with a specific harmful threat to a particular anatomical site, and are these responses localized or widely distributed? How much input is required to trigger a response and to what extent is the behavior maintained by ongoing input from the periphery? Many such questions remain

unanswered because behavioral and sensory responses to noxious stimuli are commonly applied and measured over a timescale of seconds, even though the nervous system operates in the millisecond range.

Optogenetics enables specific activation of genetically defined primary afferents in a localized area with high temporal control, but this technology had only been applied with low temporal resolution (Daou et al., 2013; Iyer et al., 2014). Recently, Lechner and colleagues used single-shot optogenetic stimulation to identify an interaction between low-threshold mechanoreceptors and A-fiber nociceptors by examining local sub-second behavioral responses at 240 frames per second (Arcourt et al., 2017). Here we examine the repertoire of behavioral responses on even faster timescales, across the whole animal. We mapped the fast, global structure of evoked responses in awake, freely-behaving animals by combined single-shot millisecond optogenetic activation of cutaneous nociceptors with millisecond (1 kHz) sampling of behavior (Figure 1A). The relative timings for regional and general responses to a single time-locked input were used to examine the nature and coordination of the behavioral output. We reveal the complexity and diversity with which the nervous system coordinates fast protective behavior across the whole animal, identifying responses that could only be observed at a millisecond timescale. Such an approach may have general utility for studying stimulus evoked behaviors.

RESULTS

Single-pulse optogenetic activation of nociceptors evokes rapid protective behaviors

We expressed the light-activated ion channel ChR2 in two broad-classes of cutaneous nociceptor afferent by crossing Cre-dependent ChR2-tdTomato mice (Madisen et al., 2012) with either TRPV1-Cre or Tac1-Cre mice (Basbaum et al., 2009; Cavanaugh et al., 2011; Harris et al., 2014). In the resultant mice, freely-behaving on a glass floor, a single pulse of blue light as short as 3 ms to the glabrous hindpaw surface caused hindlimb withdrawal in most trials (Figure 1B to D). Increasing the duration of the light stimulus increased response probability (Figure 1D). The blue light was delivered as a small 900 m spot to the hindpaw (~1% of the glabrous surface) but withdrawal still occurred with an even smaller stimulation area; 0.3% of the glabrous surface. Using a time-locked single 3 ms pulse as a reference, subsequent protective behaviors were recorded using a high-speed camera at 1 kHz to resolve the responses on a millisecond timescale. The temporal and spatial precision, and genetic specificity of this approach allowed us to map the fine-grained temporal structure of protective behaviors at the whole animal level.

First we confirmed that ChR2 expression in TRPV1::ChR2 and Tac1::ChR2 mice indeed matched the profiles for small-diameter C and Aδ nociceptors whose peripheral terminals innervated the epidermis of the skin and their central axons projected into lamina III of the spinal cord dorsal horn (Todd, 2010) (Figures 1E, and S1A to D). These ChR2-expressing DRG neurons displayed nociceptor-characteristic high-threshold and wide half-width action potentials in response to both light and current injection (Figures 1F, and S1E to G) (Fang et al., 2005; Petruska et al., 2000). Both mouse lines exhibited normal sensitivity to noxious thermal cutaneous stimuli (Figure S2A). Behavioral responses to light were evoked only by the specific optogenetic activation of afferent fibers (Figure S2B and C). TRPV1::ChR2 and

Tac1::ChR2 mice therefore represent two complementary but independent DRG nociceptor-driver lines, and in the following experiments, produced essentially identical responses.

Whole-cell patch clamp recordings from cultured DRG neurons from the two mouse lines showed that a single 3 ms pulse of light only ever generated a single action potential, which was time-locked (Figure 2A). Action potential voltage threshold and half-width were identical, whether evoked by optogenetic stimulation or current injection (Figure S1G). DRG neurons negative for ChR2-tdTomato did not display any photocurrents (8 cells).

We confirmed a similar pattern of activation *in vivo*, using loose-patch recordings from targeted DRG neurons in anesthetized mice (Figure 2B and C) (Bai et al., 2015). Only single action potentials were generated by 3 ms light stimuli to the hindpaw, with very low jitter (0.3–10.6% of unit interval, 60 trials), which reached the DRG between 6.7 and 100.7 ms after the hindpaw stimulus, indicating activation of both Aδ and C fibers.

In order to resolve the precise timing of motor reactions to the time-locked 3 ms light pulse, we recorded evoked behavior at 1 kHz in mice that were “idle” (still and awake; Figure S3) with all paws on the ground (Figure 1B, and Movies S1 and S2). The minimal latency for first observable movement of the hindlimb was 21 and 20 ms for TRPV1::ChR2 and Tac1::ChR2 mice respectively (Figures 3B, 3D and S4A). The response latencies to first paw withdrawal were distributed in two distinct millisecond-timescale populations, around 30 ms and 140 ms. These two different times likely reflect responses to the activation of Aδ or C-fibers respectively, as there is a high correspondence between these behavioral latencies and the conduction latencies obtained from *in vivo* loose-patch DRG recordings (Figure 2C). Small-diameter DRG neurons have low maximum firing frequencies and long interspike intervals (Figure 2D) and even in circumstances where a second action potential was evoked by a peripheral stimulus, this would arrive in the CNS too late – after the behavior was completed; thus, fast withdrawal behavior is triggered by arrival of the first set of single action potentials to the spinal cord. The short and the longer latency responses occurred within the same animal on different trials and may reflect either the specific population activated by a particular stimulus or the state of the CNS which may facilitate or gate different inputs, depending on the context of the stimulus.

These electrophysiological, immunohistological and behavioral experiments indicate that TRPV1-Cre and Tac1-Cre selectively target both Aδ and C fibres. Although these nociceptive fibers represents a mixture of functionally distinct sensory neuron subtypes, their optogenetic activation is much more selective than that produced by a brief electrical stimulation and without the inevitable activation of low-threshold Aβ fibres which influence nociceptive pathways (Duan et al., 2014; Melzack and Wall, 1965). The optogenetic strategy allows us to control a genetically-defined nociceptive input with single action potential resolution and examine its relationship with the behavioural output at the millisecond-timescale.

In wild type mice using the same high speed monitoring of natural stimulus-evoked behaviour, we found that thermal stimulation of the hindpaw (100 mW blue light) generated a response with a latency of 1.8 ± 0.4 s (five trials), which is much slower than that activated

by optogentic activation of TRPV1-lineage nociceptors. The delay must reflect the time taken for the skin to heat to a temperature sufficient to activate the nociceptors. Mechanical stimulation (pinprick) of the hindpaw gave a much faster response; 74 ± 12 ms (27 trials), but here it is not possible to dissociate responses evoked by activation of low threshold from high threshold mechanoreceptors and the extent of the delay caused by distribution of mechanical forces though the tissue.

Withdrawal is not invariant but timed according to context

Mice that were grooming at the time of the stimulus showed substantially reduced withdrawal probabilities (TRPV1::ChR2, 1/15 withdrawals; Tac1::ChR2, 11/42 withdrawals) suggesting that nociceptive behaviors are actively suppressed in certain contexts (Callahan et al., 2008). In sleeping TRPV1::ChR2 mice (non REM sleep, determined by EEG recording), flexion was observed in 9/20 stimuli, which reflects a reduction in withdrawal probability compared with the awake state which responded to 33/39 stimuli.

High-speed recordings reveal a diversity of responses to the same stimulus (Figure S5) and that the timing of responses was influenced by context. We found that the latency to paw withdrawal was influenced by the posture of the animal (Figures 3, and S4A and B); hindlimb withdrawal was slower in mice with forepaws raised from the floor (“forepaw-up”) compared with mice where all paws were in contact with the floor (“forepaw-down”). Cumulative distributions showed that this effect reflects a delay specifically in the slower latency putative C-fiber response, which were over two-fold slower in forepaw-up than in forepaw-down situations (K-S test $p < 0.0082$). This finding indicates that the timing of the hindlimb flexion withdrawal may be delayed to maintain balance. Consistent with this, in the forepaw-up state, the forelimb moved from its flexed position to an extended position with a fast latency, usually well before hindlimb withdrawal (Figures 3C and S4B, and Movie S1). Fast and slow hindpaw behavioral responses occurred in the forepaw-down state at about equal frequency (Figure 3E). The proportion of positive hindpaw responses was overall lower in the forepaw-up compared to the forepaw-down situation (Figure 3E). Therefore, hindlimb withdrawal can be delayed or even on some occasions prevented from occurring, perhaps to minimize the summed risk, falling or withdrawal. These findings show that the nociceptive flexion reflex is not hardwired to evoke an invariant withdrawal response at a fixed time but rather reflects an integration of diverse influences operating at a sub-second scale.

Local nociceptor activation recruits responses across the whole animal simultaneously

Single-shot hindpaw optogenetic stimulation did not only result in movements restricted to the limbs, but unexpectedly, also in coordinated movements of the whole animal. The vibrissae showed clear movements, usually well before the hindlimb withdrawal (Figures 4 and S4C, and Movies S1 and S2). The minimum latencies for vibrissae movement in TRPV1::ChR2 mice (15 ms) and Tac1::ChR2 mice (20 ms) were shorter than hindlimb flexion and indicate recruitment by Aδ afferents. No movement of vibrissae, limbs, head, body or tail was detected in response to light stimulation in eight control (no ChR2) littermate mice (25 recordings, 400 ms sampled). That a brainstem motor output occurs even

before the flexion reflex indicates that the vibrissae are part of a global protective system to very rapidly identify the spatial source of danger.

High-speed recordings show that global responses also occur with a natural noxious mechanical stimulus (pinprick). The latency for global responses in this situation occurred at 37 ± 9 ms while the stimulated hind paw responded at 104 ± 26 ms (six responses). Both low-threshold and high-threshold mechanoreceptors are activated by this stimulus. However, using optogenetics we reveal that nociceptors alone are sufficient to drive millisecond-timescale spinal segmental responses as well as ones initiated in the brain, and that the latter generally occur before the former.

Tail flick is another spinal withdrawal reflex enabling escape of this body part from potentially injurious stimuli. Single-shot optogenetic activation of the tail flick reflex initiated localized tail withdrawal response, which was concurrent with widespread movements of the vibrissae, head, body, and limbs (Figure 5 and Movie S3). Absolute latencies for tail responses were longer than for stimulation of the hindpaw, with a minimum latency of 104 ms (TRPV1, 35 recordings from 8 mice) and 110 ms (Tac1, 54 recordings from 8 mice), and means of 247 ± 9 ms and 263 ± 7 ms respectively. This provided an extended time window in which to resolve distinct global behavioral latencies. These behaviors are likely, given the latency, to be driven mainly by C-fiber input, unlike the hindpaw where we observed short and long latency responses – which may reflect different sensory innervation in these tissues. While hindlimb stimulation invariably generated short latency Aδ evoked general body (whisker) movements, the long latency of the general body movements evoked in response to tail stimulation indicate that C fibres also can access distributed alerting responses. Although like hindlimb withdrawal, the tail flick was considered to represent only a localized spinal reflex (Irwin et al., 1951), our data indicate that nociceptor activation in the tail evokes behaviors that are not limited to the spinal cord, but extend globally to produce coordinated widespread subsecond protective responses.

Sub-second awakening on minimal nociceptor activation

Cortical electroencephalography recordings during brief 3 ms optogenetic stimulation in sleeping mice showed that the stimulation provoked the mice to wake with a latency consistent with C-fiber activation (Figure 6). Input from those few nociceptors innervating a small area of hindpaw skin has therefore, widespread consequences in the CNS that include terminating sleep within a fraction of a second (156 ± 29 ms, n = 9) – an order of magnitude faster than with an innocuous acoustic tone (Kaur et al., 2013). This reveals that the sleep to wake transition can occur very rapidly in response to danger; cortical activity can be changed within a fraction of a second by a single action potential volley initiated at the skin in nociceptors.

DISCUSSION

Primary afferent nociceptors are genetically and functionally heterogeneous, allowing for discriminative detection of many somatic sensory modalities, intensities and timings, including noxious thermal, mechanical, and chemical stimuli. In an experimental setting, the controlled application of a thermal, mechanical or chemical stimulus is designed to mimic

naturalistic activation of cutaneous afferents in a real-life setting, and has been essential in studying the neural underpinnings of sensory processing. In spite of this, fundamental principles underlying nociceptor coding remain unclear, for example, the extent to which polymodal nociceptors contribute to coding (Prescott et al., 2014). One problem is that any naturalistic stimulus however brief will necessarily activate multiple subpopulations of nociceptors at different times, and in most cases low-threshold afferents also, making it difficult to define the particular consequences of specific inputs from one class of neuron. Studying some of the fundamental properties of nociceptors and the behavioral responses they evoke *in vivo* requires greater specificity and temporal control than that afforded by such naturalistic stimuli. These stimuli are typically applied at a timescale that is slower than the timescale for the nervous system to respond (millisecond). Indeed, high-threshold nociceptors do not fire until the stimulus applied to the skin tissue has reached the activation threshold of transducers on their peripheral terminals by changing the temperature of the skin, transferring force through the skin or the diffusion of chemicals to the receptors.

We used optogenetic stimulation in this study as an alternative strategy to naturalistic stimuli to both obtain genetic specificity of the class of afferent activated and to give us high temporal single action potential resolution. This approach, by bypassing the delays due to sensory transduction mechanisms, allows for direct study in the millisecond range of the central consequences of defined inputs. Our data show that optogenetic stimulation provides unique advantages for understanding the temporal relationship between a specific nociceptor input and its output, that are not possible with naturalistic stimulation. Precise control of which afferent is stimulated and when is obviously artificial in its nature, normally such a limited input is unlikely to occur, but it does enable important aspects of sensory responses to be experimentally measured. Our data showing that pinprick like optogenetic stimuli elicits global responses, indicate that the nature of the response evoked by the optogenetic stimulation does not differ qualitatively from that produced by naturalistic stimuli.

In the present study we combine high spatiotemporal resolution and minimal genetically-specific input to examine fast protective stimulus-response relationships across the whole animal in freely-behaving mice at a millisecond timescale. Nociceptors innervating skin were genetically-targeted and optically stimulated using a single short pulse of light so that the timings of behavioral responses could be resolved with a high-speed camera at 1 kHz. Combining optogenetics with millisecond timescale sampling of global behavior reveals behavioral features that otherwise could not have been observed. This strategy has provided insight into the operation of the CNS related to the initiating alerting responses to danger and the coordinating of body movement to minimise potential harm (Figure 7), but also relates to more general aspects of CNS organization at a sub-second scale.

Rodents can be trained to report on single action potentials in a few hundred neurons in the barrel cortex (Huber et al., 2008). Such associative learning can also be achieved with a train of action potentials in a single neuron in the motor cortex and somatosensory cortex (Brecht et al., 2004; Houweling and Brecht, 2008). In larval zebrafish a single action potential in a single trigeminal neuron is sufficient to drive escape behavior (Douglass et al., 2008). We find that initiation of a single action potential volley in mammalian primary sensory neurons is also sufficient to elicit robust innate protective behaviors in agreement with the recent

findings of others (Arcourt et al., 2017). The latter authors measured the resultant local segmental responses at 240 frames per second. Here we develop this approach further and exploit the time-locked single action potential input to map the precise temporal structure of the resultant fast behavior at the millisecond timescale and the whole animal level.

Over a century ago, Sherrington described the nociceptive flexion-reflex of the limb and its properties in decerebrate and spinal cat preparations; noxious stimulation of the hindlimb simultaneously activates flexor muscles and inhibits extensor muscles, to withdraw the limb from the stimulus (Sherrington, 1910; Sherrington, 1906). Forelimb reflex movements accessory to this protective reflex were also observed by Sherrington in these preparations. Here we show in freely behaving mice that movements in the vibrissae, head, body and forelimbs occur simultaneously with movement of the hindlimb. Thus information arriving in one highly spatially restricted part of the dorsal horn of the spinal cord by single action potentials in a small number of sensory fibers appears to be rapidly distributed across many different parts of the CNS to initiate multiple rapid and diverse movements. This response includes the initiation of exploratory movements by the vibrissae sensory system, which have important roles in sampling the environment (Moore, 2004) and coordinate protection of the animal. Activation of vibrissae movement was particularly highly time locked with the jitter expected of a polysynaptic circuit. The nociceptor input was also sufficient to terminate sleep within a fraction of a second. This rapid transition from sleep to wake states promotes transient arousal, potentially to prepare to flee from the stimulus source. This illustrates how widespread the circuits are that can be recruited by minimal nociceptive input.

We observe that certain behavioral responses are suppressed or delayed, depending on the ongoing state of the animal, as set by body position and activities like grooming. These findings suggest that information about body state is distributed to determine the nature and timing of any response elicited at a particular time from a particular location. How circuits run extended programs from a single action potential input and how and where interactive postural and activity gating operates, now need to be established, including where nociceptive information is stored in the CNS until movement is permitted by the relief of any gating, long after the input is over.

Taken together, our data show that the system operates like a tripwire, such that minimal input to the central nervous system triggers widespread but coordinated and interactive neural programs, that once activated become independent of any need for further afferent input. This set of widely distributed interacting circuits is far more complex than the prototypic primary nociceptive protective reflex response; a short polysynaptic chain of excitatory interneurons to ipsilateral flexor motor neurons and inhibitory interneurons to extensor motor neurons in the same spinal cord segment. The resolution afforded by combining optogenetics with global millisecond behavioral response mapping of awake behaving animals has revealed an unsuspected complexity of even the simplest of nervous system stimulus-response relationships, one that now needs to be reconciled with growing insights into the dynamic network states present in neural microcircuitry (Markram et al., 2015). We reveal that a single input in a very limited skin area drives multiple parallel innate programs distributed throughout the spinal cord, brain stem and cortex that alert the animal to and protect it from danger in a dynamic manner that reflects its current state, reinforcing

the presence in the CNS of selectable, complex and diverse sub-second behavioral responses (Wiltschko et al., 2015). The identity of the circuits that guide these dynamic sub-second responses and their influence on the experience of pain can now be investigated.

EXPERIMENTAL PROCEDURES

Further details and an outline of resources used in this work can be found in Supplemental Experimental Procedures.

Mice

Targeted expression of ChR2-tdTomato in nociceptive primary afferents was achieved by breeding heterozygous Rosa-CAG-LSL-hChR2(H134R)-tdTomato-WPRE (Ai27D) mice (Madisen et al., 2012) with mice with Cre recombinase inserted downstream of the *TRPV1* (Cavanaugh et al., 2011) or *TAC1* genes (Harris et al., 2014). The background strain was C57BL/6j. Resultant mice were heterozygous for both transgenes and were housed with control littermates. Mice were given *ad libitum* access to food and water and were housed in at 22 ± 1°C, 50% relative humidity, and a 12-hr light:12-hr dark cycle. Adult (2–6 month old) mice were used in experiments. Male and female mice were pooled by genotype to limit the number of animals used.

All experiments were carried out at Boston Children's Hospital and Harvard Medical School and were conducted according to institutional animal care and safety guidelines and with IACUC approval.

Behavioral studies

Experiments were conducted in a quiet room at 22 ± 1°C with 50% relative humidity. Animals were acclimatized to the behavioral testing apparatus during three habituation sessions in advance of starting the experiment. The behavioral tester was blinded and randomization was achieved through the breeding strategy where mice were separated based on their sex during weaning.

In vivo optogenetics

Mice were placed on a borosilicate glass (1.1 mm thick) platform in 7.5 cm × 7.5 cm × 15 cm chambers and acclimatized for at least one hour. A requirement was that the mice were in a calm and awake "idle" state and not grooming or exploring, so that there was minimal movement before optogenetic stimulation, increasing the signal-to-noise ratio. "Non-idle" states were identified as a body posture that was lowered to the floor, since these were likely not awake they were not used (Figure S3). A 473 nm DPSS laser (100 mW, LaserGlow) coupled to a multimode FC/PC optical fiber (400 μm core diameter 1 m length, Thorlabs) was used in all behavioral experiments. A computer-controlled pulse generator (OPTG-4, Doric) was used to supply TTL signals to the laser driver. Average power density was estimated by sampling 400 pulses over 20 seconds using a PS19 optical power meter (Coherent). The optical fiber tip was positioned below the left hindpaw during optogenetic stimulation (3 ms at 47 $mW.mm^{-2}$). This was consistently applied to the center of the lateral plantar glabrous surface to minimise any differences in innervation density. A 3 ms pulse

duration was selected to resolve the relatively short response times accurately. Behavior was sampled at 1,000 frames per second using an acA2040-180kmNIR cameralink CMOS camera (Basler) with an 8 mm lens and set at 500 pixels × 350 pixels under normal ambient lighting (800 μs exposure time). Light saturation was reduced by a yellow-orange lens filter. Acquisition was carried out using LabVIEW on a computer with excess buffer capacity to ensure all frames were successfully retained. An oscilloscope was used to confirm the frame rate. An Edgertronic high-speed camera was also used. All experiments used at least two independent litters and were duplicated. Hindpaw, forelimb, vibrissae, head and body latencies were determined manually frame by frame. Littermate controls without Cre recombinase, or without ChR2, never reacted to a 10 ms blue light pulse (3 trials for 15 mice). TRPV1::ChR2 and Tac1::ChR2 mice did not respond to an equivalent off-spectra pulse of light (594 nm, three trials in seven mice each for TRPV1::ChR2 and Tac1::ChR2).

Statistical Methods

Pooled data are given as the mean ± SEM unless specified otherwise. Two-tailed unpaired Student's t-test was used to compare a single measurement between two groups. Nonparametric ANOVA was used for multiple comparisons of statistical significance. In all tests $P < 0.05$ was considered significant. The glabrous hindpaw surface was 56 ± 1 mm^2 (both paws in 10 mice). The minimal latency for first observable movement of the hindlimb was 21 ms for TRPV1::ChR2 (36 trials, 13 mice) and 20 ms for Tac1::ChR2 mice (63 trials, 10 mice). The Kolmogorov-Smirnov test was used to compare cumulative distributions that were separated into fast and slow populations using a threshold of 60 ms (Figure 3). The response latencies to first paw movement were showed means of 29 ± 1 and 143 ± 24 ms (from 19 and 10 responses respectively) for TRPV1::ChR2 mice, and 32 ± 2 or 129 ± 17 ms (from 20 and 26 responses) for Tac1::ChR2 mice.

Supplementary Material

Refer to Web version on PubMed Central for supplementary material.

Acknowledgments

NIH RO1DE022912 R01NS038253, R37NS039518 (C.J.W.), R35NS97344 (D.D.G), and F32NS095631 (B.P.L.); and a Marie Curie Actions Fellowship from the European Commission (329202) and a Sir Henry Dale Fellowship jointly funded by the Wellcome Trust and the Royal Society (109372/Z/15/Z) (L.E.B.).

References

Arcourt A, Gorham L, Dhandapani R, Prato V, Taberner FJ, Wende H, Gangadharan V, Birchmeier C, Heppenstall PA, Lechner SG. Touch Receptor-Derived Sensory Information Alleviates Acute Pain Signaling and Fine-Tunes Nociceptive Reflex Coordination. Neuron. 2017; 93:179–193. [PubMed: 27989460]

Bai L, Lehnert BP, Liu J, Neubarth NL, Dickendesher TL, Nwe PH, Cassidy C, Woodbury CJ, Ginty DD. Genetic Identification of an Expansive Mechanoreceptor Sensitive to Skin Stroking. Cell. 2015; 163:1783–1795. [PubMed: 26687362]

Basbaum AI, Bautista DM, Scherrer G, Julius D. Cellular and molecular mechanisms of pain. Cell. 2009; 139:267–284. [PubMed: 19837031]

Brecht M, Schneider M, Sakmann B, Margrie TW. Whisker movements evoked by stimulation of single pyramidal cells in rat motor cortex. Nature. 2004; 427:704–710. [PubMed: 14973477]

Callahan BL, Gil AS, Levesque A, Mogil JS. Modulation of mechanical and thermal nociceptive sensitivity in the laboratory mouse by behavioral state. J Pain. 2008; 9:174–184. [PubMed: 18088557]

Cavanaugh DJ, Chesler AT, Jackson AC, Sigal YM, Yamanaka H, Grant R, O'Donnell D, Nicoll RA, Shah NM, Julius D, et al. Trpv1 reporter mice reveal highly restricted brain distribution and functional expression in arteriolar smooth muscle cells. The Journal of neuroscience: the official journal of the Society for Neuroscience. 2011; 31:5067–5077. [PubMed: 21451044]

Clarke RW, Harris J. The organization of motor responses to noxious stimuli. Brain Res Brain Res Rev. 2004; 46:163–172. [PubMed: 15464205]

Daou I, Tuttle AH, Longo G, Wieskopf JS, Bonin RP, Ase AR, Wood JN, De Koninck Y, Ribeiro-da-Silva A, Mogil JS, et al. Remote optogenetic activation and sensitization of pain pathways in freely moving mice. The Journal of neuroscience: the official journal of the Society for Neuroscience. 2013; 33:18631–18640. [PubMed: 24259584]

Douglass AD, Kraves S, Deisseroth K, Schier AF, Engert F. Escape behavior elicited by single, channelrhodopsin-2-evoked spikes in zebrafish somatosensory neurons. Curr Biol. 2008; 18:1133–1137. [PubMed: 18682213]

Duan B, Cheng L, Bourane S, Britz O, Padilla C, Garcia-Campmany L, Krashes M, Knowlton W, Velasquez T, Ren X, et al. Identification of spinal circuits transmitting and gating mechanical pain. Cell. 2014; 159:1417–1432. [PubMed: 25467445]

Fang X, McMullan S, Lawson SN, Djouhri L. Electrophysiological differences between nociceptive and non-nociceptive dorsal root ganglion neurones in the rat in vivo. The Journal of physiology. 2005; 565:927–943. [PubMed: 15831536]

Harris JA, Hirokawa KE, Sorensen SA, Gu H, Mills M, Ng LL, Bohn P, Mortrud M, Ouellette B, Kidney J, et al. Anatomical characterization of Cre driver mice for neural circuit mapping and manipulation. Frontiers in neural circuits. 2014; 8:76. [PubMed: 25071457]

Houweling AR, Brecht M. Behavioural report of single neuron stimulation in somatosensory cortex. Nature. 2008; 451:65–68. [PubMed: 18094684]

Huber D, Petreanu L, Ghitani N, Ranade S, Hromadka T, Mainen Z, Svoboda K. Sparse optical microstimulation in barrel cortex drives learned behaviour in freely moving mice. Nature. 2008; 451:61–64. [PubMed: 18094685]

Irwin S, Houde RW, Bennett DR, Hendershot LC, Seevers MH. The effects of morphine methadone and meperidine on some reflex responses of spinal animals to nociceptive stimulation. J Pharmacol Exp Ther. 1951; 101:132–143. [PubMed: 14814606]

Iyer SM, Montgomery KL, Towne C, Lee SY, Ramakrishnan C, Deisseroth K, Delp SL. Virally mediated optogenetic excitation and inhibition of pain in freely moving nontransgenic mice. Nat Biotechnol. 2014; 32:274–278. [PubMed: 24531797]

Julius D. TRP channels and pain. Annual review of cell and developmental biology. 2013; 29:355–384.

Kaur S, Pedersen NP, Yokota S, Hur EE, Fuller PM, Lazarus M, Chamberlin NL, Saper CB. Glutamatergic signaling from the parabrachial nucleus plays a critical role in hypercapnic arousal. The Journal of neuroscience: the official journal of the Society for Neuroscience. 2013; 33:7627–7640. [PubMed: 23637157]

Madisen L, Mao T, Koch H, Zhuo JM, Berenyi A, Fujisawa S, Hsu YW, Garcia AJ 3rd, Gu X, Zanella S, et al. A toolbox of Cre-dependent optogenetic transgenic mice for light-induced activation and silencing. Nature neuroscience. 2012; 15:793–802. [PubMed: 22446880]

Markram H, Muller E, Ramaswamy S, Reimann MW, Abdellah M, Sanchez CA, Ailamaki A, Alonso-Nanclares L, Antille N, Arsever S, et al. Reconstruction and Simulation of Neocortical Microcircuitry. Cell. 2015; 163:456–492. [PubMed: 26451489]

Melzack R, Wall PD. Pain mechanisms: a new theory. Science. 1965; 150:971–979. [PubMed: 5320816]

Moore CI. Frequency-dependent processing in the vibrissa sensory system. Journal of neurophysiology. 2004; 91:2390–2399. [PubMed: 15136599]

Petruska JC, Napaporn J, Johnson RD, Gu JG, Cooper BY. Subclassified acutely dissociated cells of rat DRG: histochemistry and patterns of capsaicin-, proton-, and ATP-activated currents. Journal of neurophysiology. 2000; 84:2365–2379. [PubMed: 11067979]

Prescott SA, Ma Q, De Koninck Y. Normal and abnormal coding of somatosensory stimuli causing pain. Nature neuroscience. 2014; 17:183–191. [PubMed: 24473266]

Schouenborg J, Kalliomaki J. Functional organization of the nociceptive withdrawal reflexes. I. Activation of hindlimb muscles in the rat. Exp Brain Res. 1990; 83:67–78. [PubMed: 2073951]

Schouenborg J, Weng HR. Sensorimotor transformation in a spinal motor system. Exp Brain Res. 1994; 100:170–174. [PubMed: 7813646]

Sherrington CS. Flexion-reflex of the limb, crossed extension-reflex, and reflex stepping and standing. The Journal of physiology. 1910; 40:28–121. [PubMed: 16993027]

Sherrington, CSS. Integrative action of the nervous system. New Haven: Yale U.P; 1906.

Todd AJ. Neuronal circuitry for pain processing in the dorsal horn. Nature reviews Neuroscience. 2010; 11:823–836. [PubMed: 21068766]

Wiltschko AB, Johnson MJ, Iurilli G, Peterson RE, Katon JM, Pashkovski SL, Abraira VE, Adams RP, Datta SR. Mapping Sub-Second Structure in Mouse Behavior. Neuron. 2015; 88:1121–1135. [PubMed: 26687221]

Woolf CJ. Evidence for a central component of post-injury pain hypersensitivity. Nature. 1983; 306:686–688.

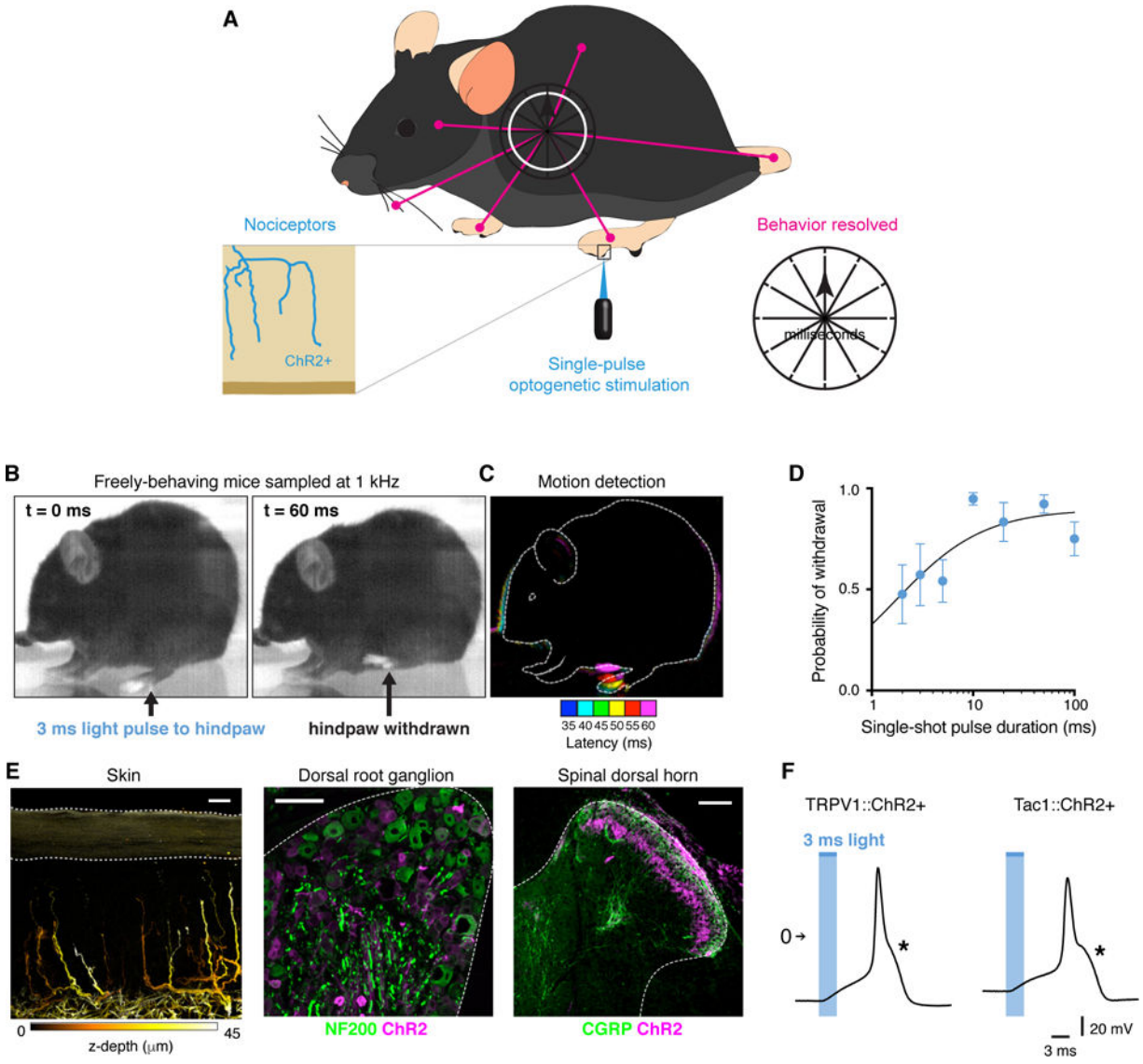

Figure 1. Rapid protective behavior time-resolved using single-pulse optogenetic activation and high-speed sampling

(A) Schematic illustrating the strategy used to map the fine-grained evoked behavioral responses with millisecond resolution. (B) Behavior elicited by a 3 ms light pulse to the hindpaw to monitor the nature, extent, timing and coordination of limb movements associated with flexion withdrawal using a camera recording at 1000 frames per second. TRPV1::ChR2 is shown. (C) Motion detected by comparing the difference in pixel intensity between frames. Each colour represents the position of the animal at a point in time. First motion was detected 35 ms from start of the 3 ms optogenetic stimulus. (D) Probability of flexion withdrawal depended on pulse duration (4 TRPV1::ChR2 mice; 6–10 trials each). Data are represented as mean ± SEM. (E) ChR2 was expressed in nociceptors that innervate the skin and spinal cord, as shown here for TRPV1::ChR2. Scale 20 μm. (F) Current-clamp recordings of cultured DRG neurons show that a 3 ms pulse of light generates a high-threshold action potential with a pronounced shoulder, as indicated by asterisk.

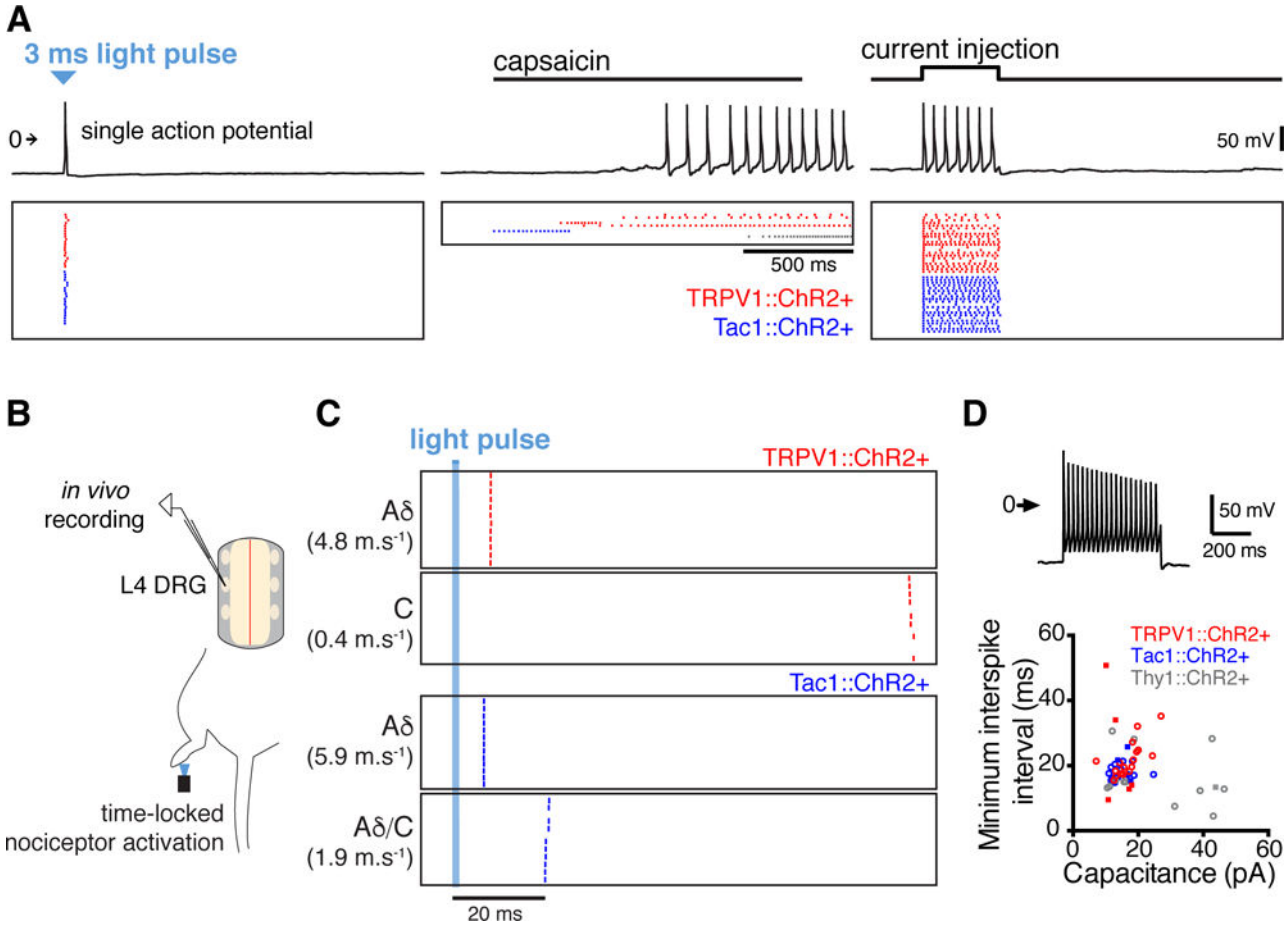

Figure 2. A single action potential volley is sufficient to drive nociceptive behavior

(A) Electrophysiological recordings (top) of a single DRG neuron (TRPV1::ChR2+) shows that one light pulse generates a single action potential, unlike activity evoked by capsaicin (1 μM). Recordings from multiple DRG neurons, plotted as action potential rasters (bottom) evoked by light, capsaicin, or current injection. Each row represents a different neuron. (B) Optogenetic stimulation in an *in vivo* cell-attached recording preparation. The plantar surface of hindpaw was illuminated with a light stimulus, eliciting an action potential that propagated centrally. (C) Rasters showing spiking response of four DRG neurons over successive trials. In all cases, the light pulse elicited only single, low jitter action potentials (0.3–10.6% of unit interval, 60 trials). Conduction velocities estimated by a distance between skin and soma of 40 mm. (D) *In vitro* whole-cell patch clamp recordings showing that small-diameter DRG neurons have low maximum firing frequencies. Current was injected in 50 pA increments up to 950 pA to identify the minimum interspike interval. A recording from a TRPV1::ChR2+ neuron injected with 950 pA is shown (top). The minimum interspike interval was plotted against the capacitance (bottom) for 24 TRPV1::ChR2+ neurons, 17 Tac1::ChR2+ neurons, and 21 Thy1::ChR2+ neurons. Thy1::ChR2+ neurons represent a mixed population of small-and large-diameter neurons. Square symbols indicate neurons that also responded to capsaicin (1 μM).

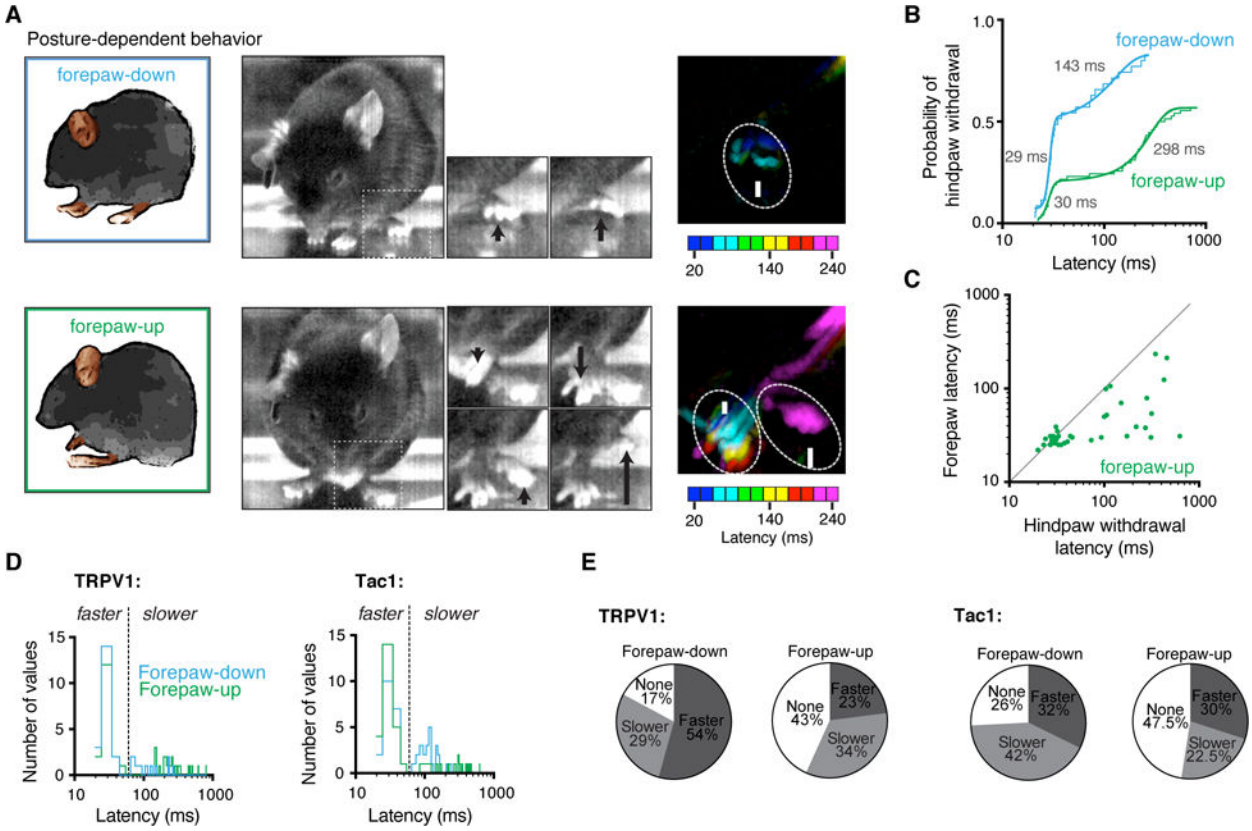

Figure 3. Rapid nociceptive behaviors are coordinated according to context

(A) Representative recordings showing postural-dependent nociceptive behaviors recorded from the same animal on the same day. The difference in pixel intensity between frames 20 ms apart illustrates the shift in timings. (B) Cumulative distributions of hindpaw withdrawal latencies reveal a short response latency in about half the trials and a much slower latency in the others, which is further delayed with forepaw-up. TRPV1::ChR2 is shown for simplicity, see Fig. S4 for Tac1::ChR2. Means are in gray. (C) Relative timings for nociceptive hindpaw withdrawal and forepaw extension in response to light in forepaw-up situation. Most responders are below unity indicating hindlimb flexion occurring after forepaw extension in forepaw-up state. TRPV1::ChR2 is shown, see Fig. S4 for Tac1::ChR2. (D) Probability distributions (10 ms bins) for hindpaw withdrawal latency in response to 3 ms optogenetic stimulation in TRPV1::ChR2 and Tac1::ChR2. Cumulative distribution fits (see B and Figure S4A) indicate that the hindpaw withdrawal occurs with two populations. These faster and slower populations were clearly separated at 60 ms (shown by the dashed line), which was used as a cutoff for statistical analysis. (E) Percentage of trials leading to no response (none), a fast latency (faster) or slow latency (slower) response showing that in forepaw-up state the hindpaw withdrawal was either slowed or less likely to occur.

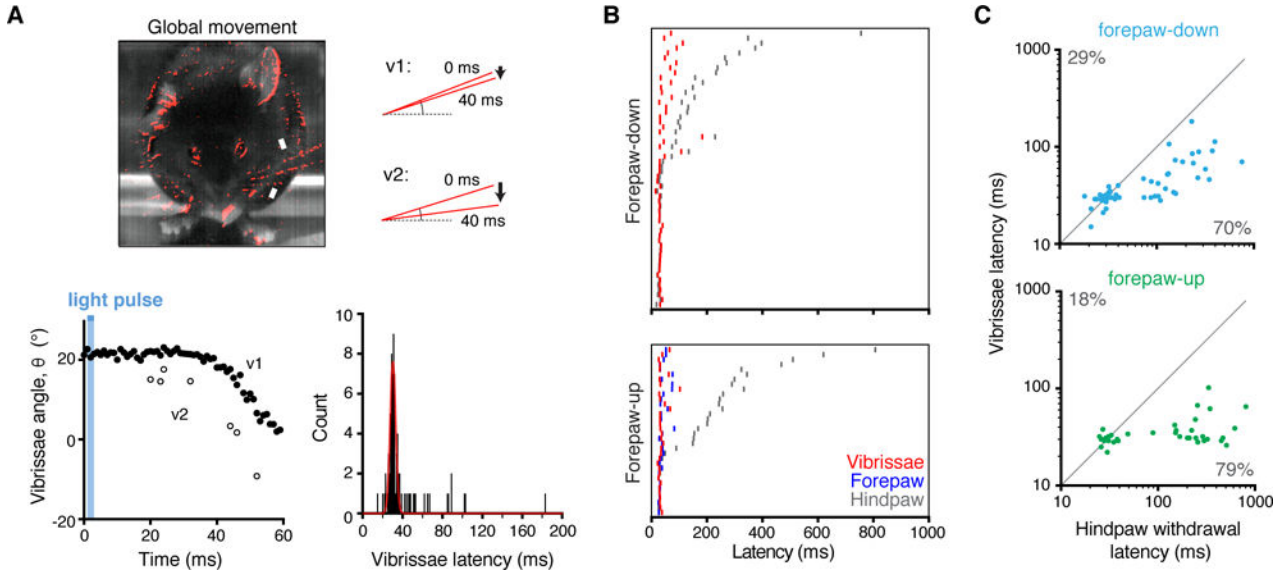

Figure 4. Global protective behavioral responses occur simultaneously

(A) Global movements of the whole animal, shown in red, detected by taking average pixel intensity of ten frames (at 1 kHz) directly before the stimulus and subtracting pixel intensity of ten consecutive frames beginning 40 ms after stimulus. Downward deflection of vibrissae is clearly resolved (top right, bottom left). The latencies for vibrissae movement fit a Gaussian curve centring on 30 ms (bottom right, 78 recordings). (B) Rasters for relative latencies for hindpaw withdrawal, forepaw movement, and vibrissae movement showing no change in vibrissae but delayed hindpaw movement in forepaw-up state. (C) Relative timings of hindpaw and vibrissae movement in response to light, revealing earlier movement of vibrissae in most cases. TRPV1::ChR2 is shown for simplicity, see Fig. S4 for Tac1::ChR2.

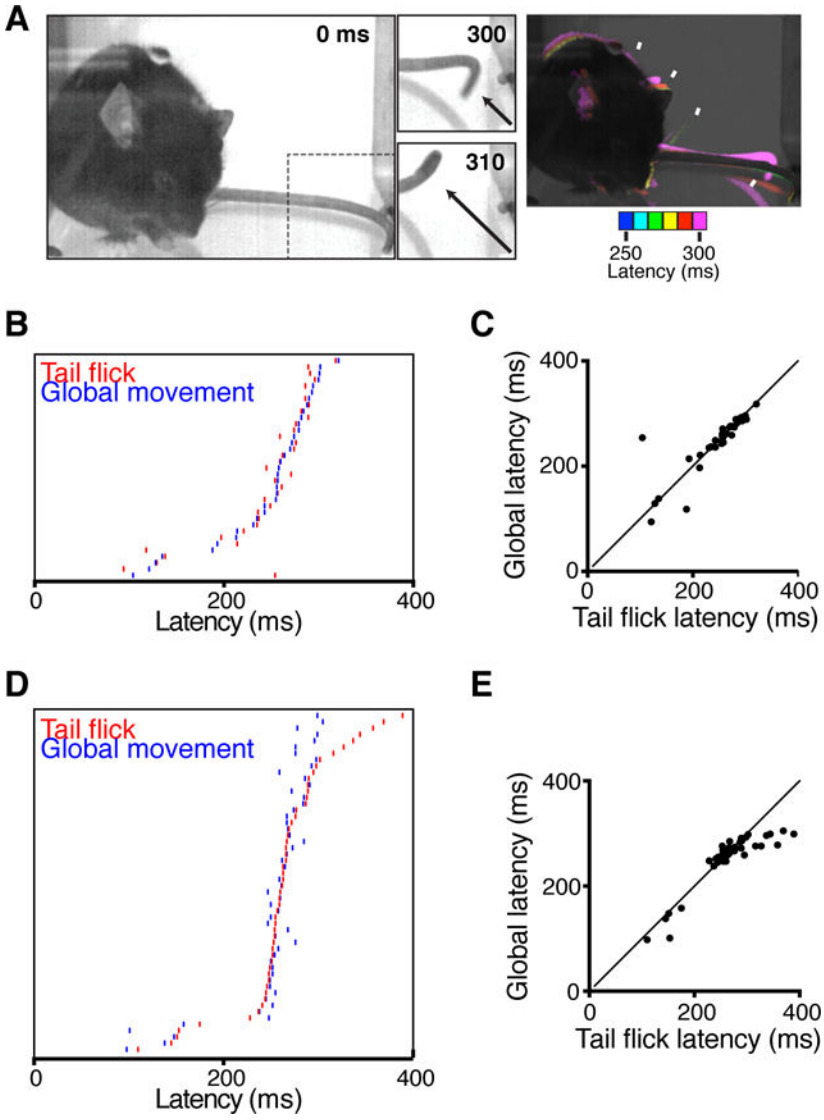

Figure 5. Time-resolved tail flick reflex

(A) A 3 ms pulse of light to distal tail tip drove coincident local tail movement and global protective behaviors. Difference in pixel intensity at 10 ms intervals illustrate relative latencies is shown on the right for a TRPV1::ChR2 mouse, as an example. (B) Rasters showing similar latencies for tail flick and global movements (vibrissae, head and body) in TRPV1::ChR2 mice. (C) Relative timings of TRPV1::ChR2 tail flick and global movements in response optogenetic stimulation (35 recordings). Slope = 0.99, Pearson's r = 0.85. (D) Raster plot showing coincident timings of optogenetically-evoked tail flick and global movements (vibrissae, head and body) in Tac1::ChR2 mice. (E) Relative timings of Tac1::ChR2 tail flick and global movements in response optogenetic stimulation (n = 54). Slope = 0.96, Pearson's r = 0.89.

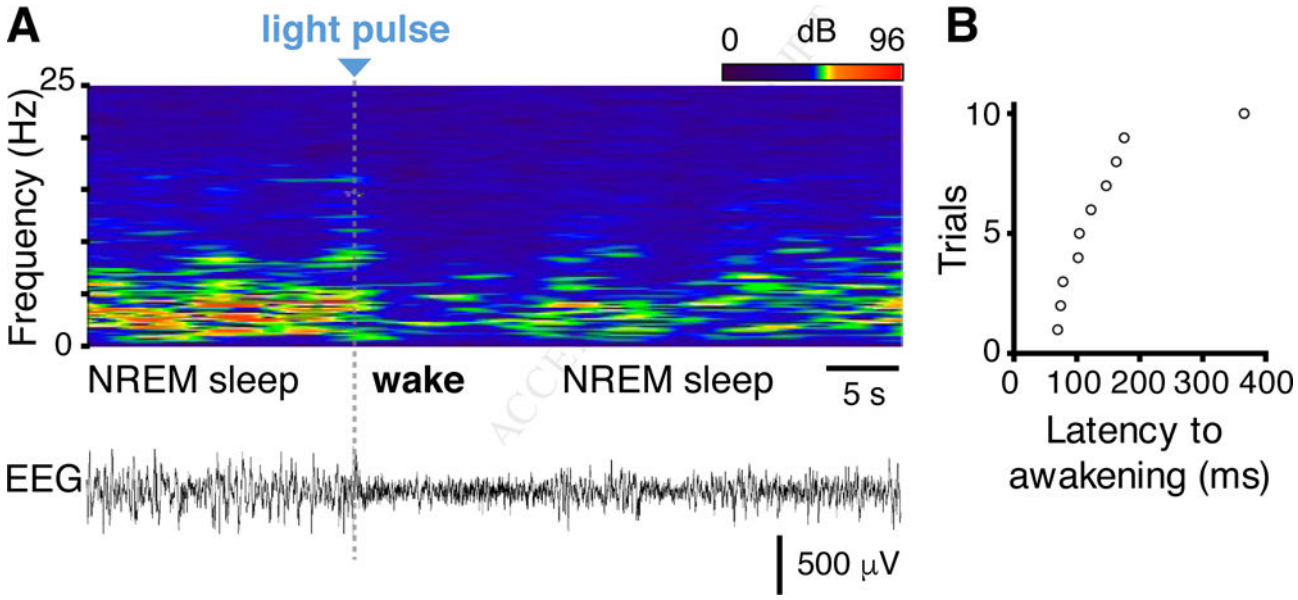

Figure 6. Minimal nociceptor activation causes sub-second awakening

(A) Latency to awakening in response to optogenetic stimulation applied to TRPV1::ChR2 mice during NREM sleep detected by EEG/EMG analysis. Top, heatmap representation of EEG power spectrogram (0–25 Hz). Bottom, corresponding EEG trace. The grey bar represents the 3 ms stimulation. Note that the animal woke with a very short latency and resumed sleep quickly. (B) Latency to awakening from NREM sleep after stimulation in 10 trials.

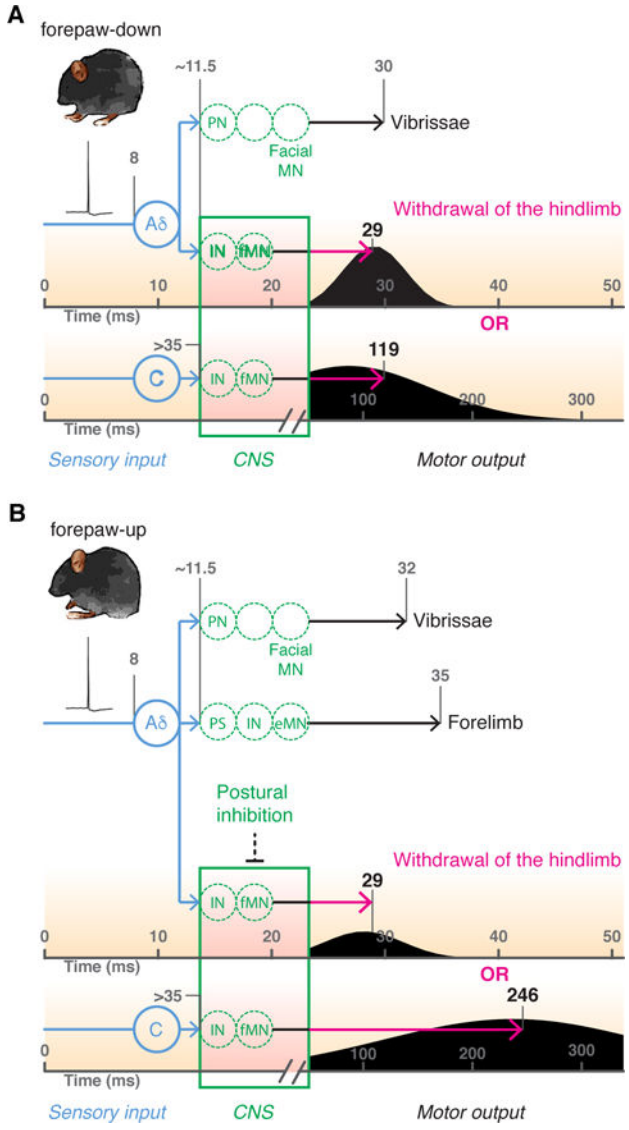

Figure 7. Model of context-dependent flexion reflex gating

Brief optogenetic activation of hindpaw nociceptors (in blue) generates a single action potential volley in Aδ and C-fibers that travel at ~5 m.s^{-1} and <1.5 m.s^{-1} respectively to reach spinal cord at ~11.5 and >35 ms. In forepaw-down state (A) the afferent input drives spinal interneurons (IN) to activate flexor motor neurons (fMN) in the ventral horn leading to hindlimb flexion. Normalised probability distributions (black curves) calculated from first derivate of fits in Fig. 3B with median latency values. Aδ nociceptors simultaneously activate projection neurons to recruit activity in supraspinal motor neurons that control vibrissae movement. In forepaw-up state (B) the Aδ response is unchanged in time although reduced in frequency but the C-fiber response is delayed or absent; in this postural position, hindlimb flexor motor neurons are tonically inhibited. Noc = nociceptor; PN = projection neuron; IN = interneuron; PS = propriospinal neuron connecting lumbar and cervical circuits; MN = motor neuron, where fMN is flexor and eMN is extensor. Calculations were based on 1) distance between the glabrous skin of the hindpaw to DRG ~40 mm; 2) distance

between the DRG and spinal cord ~10 mm; 3) synaptic delay ~1.5 ms; 4) MN conduction, neuromuscular junction delay and excitation contraction coupling ~ 7 ms.